Impact of Dynamic ^{18}F-FDG PET on the Early Prediction of Therapy Outcome in Patients with High-Risk Soft-Tissue Sarcomas After Neoadjuvant Chemotherapy: A Feasibility Study

Antonia Dimitrakopoulou-Strauss[1], Ludwig G. Strauss[1], Gerlinde Egerer[2], Julie Vasamiliette[1], Gunhild Mechtersheimer[3], Thomas Schmitt[2], Burkhard Lehner[4], Uwe Haberkorn[1,5], Philipp Stroebel[6], and Bernd Kasper[2]

[1]Medical PET Group–Biological Imaging, Clinical Cooperation Unit Nuclear Medicine, German Cancer Research Center, Heidelberg, Germany; [2]Department of Internal Medicine V, University of Heidelberg, Heidelberg, Germany; [3]Institute of Pathology, University of Heidelberg, Heidelberg, Germany; [4]Orthopedic University Hospital of Heidelberg, Heidelberg, Germany; [5]Division of Nuclear Medicine, University of Heidelberg, Heidelberg, Germany; and [6]Institute of Pathology, University Medical Center Mannheim, University of Heidelberg, Heidelberg, Germany

Dynamic PET (dPET) studies with ^{18}F-FDG were performed in patients with soft-tissue sarcomas who received neoadjuvant chemotherapy early in the course of therapy. The goal of the study was to evaluate the impact of early dPET studies and assess their value with regard to the therapy outcome using histopathologic data. **Methods:** The evaluation included 31 patients with nonmetastatic soft-tissue sarcomas, who were treated with neoadjuvant chemotherapy consisting of etoposide, ifosfamide, and doxorubicin. Patients were examined before the onset of therapy and after the completion of the second cycle. Histopathologic response served for reference and was available for 25 of 31 patients. Response was defined as less than 10% viable tumor tissue in the resected tumor tissue. The following parameters were retrieved from dPET studies: standardized uptake value (SUV); fractal dimension; 2-compartment model with computation of K_1, k_2, k_3, and k_4 (unit, 1/min); fractional blood volume; and influx according to Patlak. **Results:** The mean SUV was 4.6 before therapy and 2.8 after 2 cycles. The mean influx was 0.059 before therapy and 0.043 after 2 cycles. The mean SUV was 3.9 in the responders and 5.5 in the nonresponders before therapy. After therapy, responders revealed a mean SUV of 2.5, whereas nonresponders had a mean SUV of 3.5. We used linear discriminant analysis to categorize the patients into 2 groups: response ($n = 12$) and nonresponse ($n = 13$). The correct classification rate of the responders (positive predictive value) was generally higher (>67%) than that for the nonresponders. Finally, the combined use of the 2 predictor variables, namely SUV and influx, of each study led to the highest accuracy of 83%. This combination was particularly useful for the prediction of responders (positive predictive value, 92%). The use of the percentage change in maximum SUV led to an accuracy of 58%. **Conclusion:** On the basis of these results, only a multiparameter analysis based on kinetic ^{18}F-FDG data of a baseline study and after 2 cycles is helpful for the early prediction of chemosensitivity in patients with soft-tissue sarcomas receiving neoadjuvant chemotherapy.

Key Words: ^{18}F-FDG; sarcomas; kinetic modeling; therapy monitoring; prognosis

J Nucl Med 2010; 51:551–558
DOI: 10.2967/jnumed.109.070862

Soft-tissue sarcomas (STS) are a heterogeneous group of connective-tissue tumors that commonly arise in the extremities and constitute less than 1% of all adult malignancies (*1*). Sarcoma-related mortality from extremity lesions occurs most commonly secondary to hematogenous metastasis (*2*). Curative treatment of STS requires complete surgical resection of the primary tumor, which is not always possible. Combined treatment protocols including neoadjuvant chemotherapy (NAC) are in use in many centers as a part of a treatment plan, particularly in patients with primary STS in the extremities. The theoretic considerations for using NAC are earlier treatment of microscopic metastatic disease and facilitation of tumor removal. However, the value of neoadjuvant treatment remains unproven. Furthermore, it is known that only a subcollective of patients benefits from NAC; therefore, there is an urgent need for sensitive methods, which allow an early identification of NAC responders.

Received Sep. 18, 2009; revision accepted Dec. 10, 2009.
For correspondence or reprints contact: Antonia Dimitrakopoulou-Strauss, Medical PET Group–Biological Imaging (E0601), Clinical Cooperation Unit Nuclear Medicine, German Cancer Research Center, Im Neuenheimer Feld 280, D-69120 Heidelberg, Germany.
E-mail: ads@ads-lgs.de or a.dimitrakopoulou-strauss@dkfz.de

PET with ^{18}F-FDG is being used increasingly, primarily in patients with solid tumors for staging and therapy monitoring. The idea is that the reduction in ^{18}F-FDG uptake after chemotherapy indicates a response and a better patient outcome and that, beyond this, the change in ^{18}F-FDG uptake is a more sensitive criterion for the change in tumor volume. However, it is known that the use of ^{18}F-FDG PET for the assessment of therapeutic response is a complex topic that is still under evaluation because of the lack of widely accepted standardized protocols concerning the data acquisition and evaluation. The results of monitoring studies may vary, depending on the methodology used and the selection of the time point for the follow-up study.

The purpose of this study was to examine whether a baseline or an early ^{18}F-FDG follow-up study after the completion of the second cycle of a combined chemotherapy with etoposide, ifosfamide, and doxorubicin (Adriamycin; Pfizer Pharma) (EIA) is helpful for the prediction of the therapy outcome of NAC. Furthermore, another aim was to establish a methodology that can be used for the selection of those patients who may benefit from EIA therapy early in the treatment course, given the fact that only a portion of patients responds to NAC. The comparison of the PET ^{18}F-FDG data to clinical risk parameters was not topic of this article.

MATERIALS AND METHODS

This prospective study includes 31 patients with primary nonmetastatic histologically proven STS. All patients received combined NAC consisting of etoposide (125 mg/m^2 on days 1 and 4), ifosfamide (1,500 mg/m^2 on days 1 through 4), and doxorubicin (50 mg/m^2 on day 1) (EIA regimen, 4–6 cycles). The included patients were not diabetic and had not had previous chemotherapy. All patients were examined before the onset of chemotherapy and after the completion of the second cycle. Patients gave written informed consent to participate in the study and to have their medical records released. The study was approved by the Ethical Committee of the University of Heidelberg.

The histopathologic data were correlated to the PET data. Relevant patient data are demonstrated in Table 1. Histopathologic response data were available in 25 of 31 patients. Three patients

TABLE 1. Patients' Characteristics

Patient no.	Histology and grade	Lesion location in PET	Cycles of EIA	Resection before EIA	Response Evaluation Criteria in Solid Tumors	Histopathologic response (<10% viable cells)	Treatment after EIA
1	Synovial sarcoma, II	Upper leg	4	R1	CR	Response	R0 + IORT
2	Leiomyosarcoma, III	Upper leg	4	R1	PR	Response	R0 + IORT
3	Synovial sarcoma, III	Mediastinum	6	R2	SD	No surgery	RTx
4	Liposarcoma, III	Retroperitoneum	6	R2	SD	Response	R1 + IORT
5	Fibrosarcoma, III	Upper leg	4	R1	CR	Response	R0 + IORT
6	Fibrosarcoma, II	Upper leg	2	R2	SD	Nonresponse	R0
7	Fibrosarcoma, II	Upper leg	4	No	SD	NA	R0 + IORT
8	Synovial sarcoma, II	Upper arm	4	R1	CR	Response	R0 + IORT
9	Liposarcoma, II	Upper leg	5	No	PR	Response	R0
10	Liposarcoma, III	Thyroid gland	4	R2	PR	Response	R1
11	Epitheloid sarcoma, III	Arm/shoulder	4	No	PR	Response	R0 + RTx
12	Liposarcoma, III	Thoracic wall	4	R0	SD	No surgery	No surgery
13	MFH, III	Thoracic wall	4	No	SD	Nonresponse	R0 + IORT
14	Liposarcoma, II	Upper leg	4	No	SD	Nonresponse	R1 + RTx
15	Rhabdomyosarcoma, II	Sinus maxillaris	4	No	PR	Response	R1
16	MFH, II	Lower leg	5	No	PR	Nonresponse	R1
17	Haemangiopericytoma, II	Pelvic area	8	No	SD	No surgery	No surgery
18	Liposarcoma, III	Upper leg	4	No	SD	Nonresponse	R0 + IORT
19	Liposarcoma, III	Retroperitoneum	4	No	SD	Nonresponse	R1 + IORT
20	Liposarcoma, II	Upper leg	4	No	SD	Nonresponse	R0 + IORT
21	MFH, III	Upper leg	4	No	SD	Nonresponse	Rx + IORT
22	Synovial sarcoma, III	Pelvic area	4	No	SD	Nonresponse	R1 + IORT
23	Synovial sarcoma, III	Upper leg	4	R2	PR	Response	R0 + IORT
24	Leiomyosarcoma, III	Thoracic wall	4	R0–1	PD	Nonresponse	R0 + IORT
25	Synovial sarcoma, III	Upper leg	4	No	SD	NA	R0 + IORT
26	Liposarcoma, II	Upper leg	4	No	SD	Nonresponse	R0 + IORT
27	Liposarcoma, II	Upper leg	4	No	SD	Response	R0 + IORT
28	Synovial sarcoma, III	Lower leg	4	No	SD	Nonresponse	R0 + IORT
29	Liposarcoma, III	Upper leg	2	No	PD	Response	R0 + IORT
30	MFH, III	Upper leg	4	No	SD	NA	R0 + IORT
31	Liposarcoma, II	Upper leg	4	No	SD	Nonresponse	R0 + IORT

R1 = R1 resection; CR = complete responder; R0 = R0 resection; IORT = intraoperative radiation treatment; PR = partial responder; R2 = R2 resection; SD = stable disease; RTx = radiation treatment; NA = not applicable; MFH = malignant fibrous histocytoma; Rx = Rx resection; PD = progressive disease.

refused surgery. Response was defined as less than 10% viable tumor tissue in the resected tumor tissue. The histologic tumor response was assessed using the Salzer-Kuntschik classification (*3*). This classification system was initially developed to grade therapy-induced tumor regression of osteosarcomas but has subsequently also been used for soft-tissue tumors. The classification is based on a semiquantitative scoring of viable and necrotic tumor in a given sample. Regression grade I is defined as no viable tumor, grade II as single viable tumor cells only, grade III as less than 10% viable tumor, grade IV as 10%−50% viable tumor, grade V as more than 50% viable tumor, and grade VI as 100% viable tumor. The grade classification of tumor response was determined by a pathologist. Histologic response was defined as less than 10% viable tumor tissue in the resected tumor tissue (corresponding to grades I–II).

Dynamic PET (dPET) studies were performed over the primary tumor for 60 min after the intravenous application of 300–370 MBq of ^{18}F-FDG using a 28-frame protocol (10 frames of 30 s, 5 frames of 60 s, 5 frames of 120 s, and 8 frames of 300 s). Additional static images were acquired in all patients by moving the table in cranial and caudal positions in relation to the initial position. The gap used for each repositioning was 13.5 cm. A dedicated PET system (ECAT EXACT HR+; Siemens Co.) with an axial field of view of 15.3 cm, operated in septa-extended (2-dimensional) mode, was used for patient studies. The system allowed the simultaneous acquisition of 63 transversal slices with a theoretic slice thickness of 2.4 mm. For attenuation correction of the acquired dynamic emission tomographic images, a transmission scan for a total of 10 min was obtained before radionuclide application. A transmission scan of 3 min, followed by an emission scan of 7 min, was acquired for each additional static image. All PET images were attenuation-corrected, and an image matrix of 256 × 256 pixels was used for iterative image reconstruction. The reconstructed images were converted to standardized uptake value (SUV) images (*4*). The SUV 55–60 min after injection was used for the analysis of the ^{18}F-FDG uptake.

dPET data were evaluated using the software package PMod (PMOD Technologies Ltd.) (*5,6*). Two experienced nuclear medicine physicians visually analyzed the hypermetabolic areas on transaxial, coronal, and sagittal images.

All patients had a diagnostic MRI before the first PET study. Generally, the quantitative evaluation was based on irregular volumes of interest (VOIs) placed over the tumor and an arterial vessel within the field of view and in reference tissue (mostly the muscle in the contralateral side). For the better delineation of the tumor tissue and the improved detection of hypermetabolic lesions, parametric images were calculated on the basis of the dPET data by fitting a linear regression function to the time–activity data for each voxel. Details of this method have been described elsewhere (*7*). Parametric images of the distribution volume have been used for better anatomic delineation of the vessels. Time–activity curves were created using VOIs. A VOI consisted of several regions of interest (ROIs) over the target area. Irregular ROIs were drawn manually. To compensate for possible patient motion during the acquisition time, the original ROIs were visually repositioned but not redrawn. A detailed quantitative evaluation of tracer kinetics requires the use of compartment modeling. A 2-tissue-compartment model is the standard methodology for the quantification of dynamic ^{18}F-FDG studies (*8,9*).

One problem in patient studies is the accurate measurement of the input function, which theoretically requires arterial blood sampling. However, the input function can be retrieved from the image data with good accuracy (*10*). For the input function, the mean value of the VOI data obtained from a large arterial vessel was used. A vessel VOI consisted of at least 7 ROIs in sequential PET images. The recovery coefficient is 0.85 for a diameter of 8 mm and for the system described above. Partial-volume correction was performed in selected cases for small vessels or lesions (diameter, <8 mm) on the basis of phantom measurements of the recovery function using the PMod software. Noise in the input curve affects the parameter estimates. Therefore, we used a preprocessing tool, available in the PMod software, that allowed a fit of the input curve, namely by a sum of up to 3 decaying exponentials to reduce noise. The constants K_1–k_4 were calculated using a 2-compartment model implemented in the PMod software, taking into account the vascular fraction (VB) in a VOI as an additional variable. Details about the applied compartment model are described by Burger and Buck (*5*).

One major advantage of the PMod software is the graphical interface that allowed the interactive configuration of the kinetic model by the user and the application of some preprocessing steps, for example, setting up initial values and limits for the fit parameters. Each plot was evaluated visually to check the quality of fit. Each model curve was compared with the corresponding time–activity curve, and the total χ^2 difference was used as the cost function, for which the criterion was to minimize the summed squares (χ^2) of the differences between the measured and the model curve (χ^2 was usually <2). This means that the squared residuals (measured value minus estimated value) are multiplied by weights. In theory, the weight should be related to the SE of a measurement. The distribution at each individual point is taken to be gaussian, with an SD to be specified. The residual covariance was dependent on the kinetic parameter and typically less than 10% for K_1. The model parameters were accepted when VB and K_1–k_4 were less than one and the VB values exceeded zero. The unit for the rate constants K_1–k_4 is 1/min, and VB reflects the fraction of blood within the evaluated volume. After compartment analysis, we calculated the global influx of ^{18}F-FDG from the compartment data using the formula influx = $(K_1 \times k_3)/(k_2 + k_3)$.

In addition to the compartment analysis, a noncompartment model based on the fractal dimension (FD) was used. The FD is a parameter for the heterogeneity and was calculated for the time–activity data in each individual voxel of a VOI. The values of the FD vary from 0 to 2, showing the deterministic or chaotic distribution of the tracer activity. We used a subdivision of 7 × 7 and a maximal SUV of 20 for the calculation of FD (*11*).

Parametric images were calculated using dPET data by fitting a linear regression function to the time–activity data and for each pixel. Images of the slope and the intercept of the time–activity data have been calculated using PMod software. Parametric images of the slope reflect the trapping of ^{18}F-FDG and have been used for the delineation of the malignant lesions and the VOIs placement because of high contrast to the surrounding tissue. Parametric images of the intercept reflect the distribution volume of ^{18}F-FDG and have been used for the better anatomic localization of the lesions because of the delineation of the vessels.

Data were statistically evaluated using the STATA/SE 10.1 (StataCorp) software on a Quad-Core Intel Xeon (2 × 3.0 GHz, 16 GB RAM) running with Mac OS X 10.5.8 (Apple Computer International). The statistical evaluation was performed using the descriptive statistics, box plots, and Wilcoxon matched-pairs signed rank test. The results were considered significant for

P less than 0.1. Linear discriminant analysis with equal prior probabilities has been applied to the data.

RESULTS

The patient characteristics and individual survival data are presented in Table 1. Twenty-one patients had a primary tumor in the extremities ($n = 17$ in the upper legs, $n = 2$ in the lower legs, and $n = 2$ in the upper arms/shoulder), 1 patient in the mediastinum, 2 patients in the retroperitoneal area, 1 patient in the thyroid gland, 3 patients in the thoracic wall and axilla, 1 patient in the sinus maxillaris, and 2 patients in the pelvic area. Eighteen of the patients had a grade III tumor, and the remaining 13 patients had a grade II tumor. The diagnostic examinations performed before PET were MRI or CT. The focal ^{18}F-FDG findings were correlated to the external CT or MRI findings using a site-by-site analysis.

In 3 of 31 patients, surgery could not be performed. Of the remaining 28 patients, 23 patients received a surgical resection, followed by radiation therapy, in most cases intensity-modulated radiation therapy. Five patients refused adjuvant radiation therapy.

All tumors demonstrated an enhanced ^{18}F-FDG uptake in the baseline study. The evaluation of the follow-up ^{18}F-FDG study was in some cases more difficult than that of the baseline study. To delineate the tumor and to use VOIs comparable to those used in the baseline study, we imported the VOIs of the baseline study and adjusted the original VOIs to the follow-up study. Parametric images based on the regression function have been used for the placement of VOIs and for both studies, to better delineate the tumors and evaluate the tumor areas with the highest metabolic activity. For this purpose, the slope images have been used.

Figure 1 demonstrates an example of a patient with a grade II liposarcoma of the left upper leg, who did not respond to NAC (4 cycles EIA). The kinetic data revealed a decrease in mean SUV from 12.76 to 3.33 (73%), a decrease in k_3 from 0.104 to 0.037, and almost constant values for K_1 (baseline, 0.9; follow-up, 0.8) and VB (baseline, 0.132; follow-up, 0.085). The restaging data after 4 cycles EIA indicated stable disease; the histopathologic data, however, revealed no response to EIA (viable tumor cells $> 90\%$).

Figure 2 demonstrates an example of a patient with a grade III epitheloid sarcoma in the right upper arm/shoulder, who responded to NAC (4 cycles EIA). The kinetic data revealed a decrease in mean SUV from 9.04 to 1.63 (82%), a decrease in k_3 (baseline, 0.161; follow-up, 0.099), and a decrease in K_1 (baseline, 0.442; follow-up, 0.084) and VB (baseline, 0.113; follow-up, 0.044). The restaging data after 4 cycles of EIA indicated a partial remission, and the histopathologic data revealed a response to EIA ($<5\%$ viable tumor tissue).

Comparison Between First and Second Studies

The mean SUV was 4.6 before therapy and 2.8 after 2 cycles in all evaluated patients ($n = 31$) (Supplemental Table 1a; supplemental materials are available online only at http://jnm.snmjournals.org). The mean influx was 0.059 before therapy and 0.043 after 2 cycles ($n = 31$). The mean SUV was 3.9 in the group of responders ($n = 12$) and 5.5 in the group of nonresponders ($n = 13$) before therapy. Responders revealed a mean SUV of 2.5 after therapy, as compared with 3.5 SUV for nonresponders.

Most kinetic parameters demonstrated only small changes, typically declining after 2 chemotherapeutic cycles. The changes in the kinetic parameters were analyzed by the Wilcoxon matched-pairs signed rank test. The test revealed a significant change for K_1 ($P = 0.0735$), k_4 ($P = 0.0734$), and FD ($P = 0.0941$) when the absolute values of the first and the second studies were compared (Supplemental Table 1a). The comparison of the kinetic parameters between the first and the second PET studies with respect to histopathologic response ($n = 25$) revealed statistically significant differences only for the study after therapy for K_1 ($P = 0.0735$), k_4 ($P = 0.0734$), and FD ($P = 0.0941$) (Supplemental Table 1b). Figures 3, 3A−3C demonstrate box-and-whisker plots of the median values for all kinetic parameters before and after therapy in responders and nonresponders.

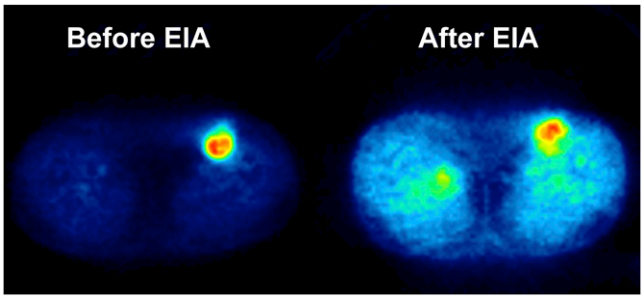

FIGURE 1. Transversal ^{18}F-FDG PET image before EIA therapy in patient with grade II liposarcoma in medioventral part of upper leg, and corresponding ^{18}F-FDG image of same patient after 2 cycles of EIA. Histopathologic data revealed no response to EIA (>90% viable tumor cells).

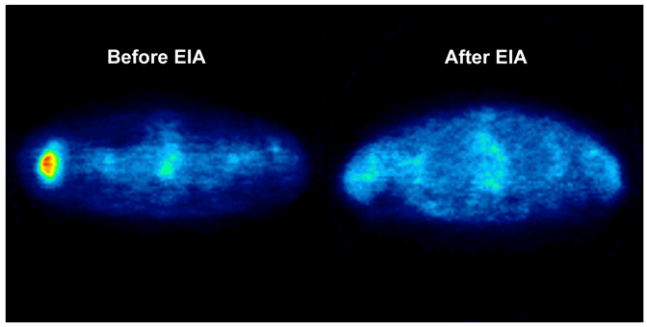

FIGURE 2. Transversal ^{18}F-FDG PET image before EIA therapy in patient with grade III epitheloid sarcoma in right upper arm/shoulder, and corresponding ^{18}F-FDG image of same patient after 2 cycles of EIA. Histopathologic data revealed a response to EIA (<5% viable tumor tissue).

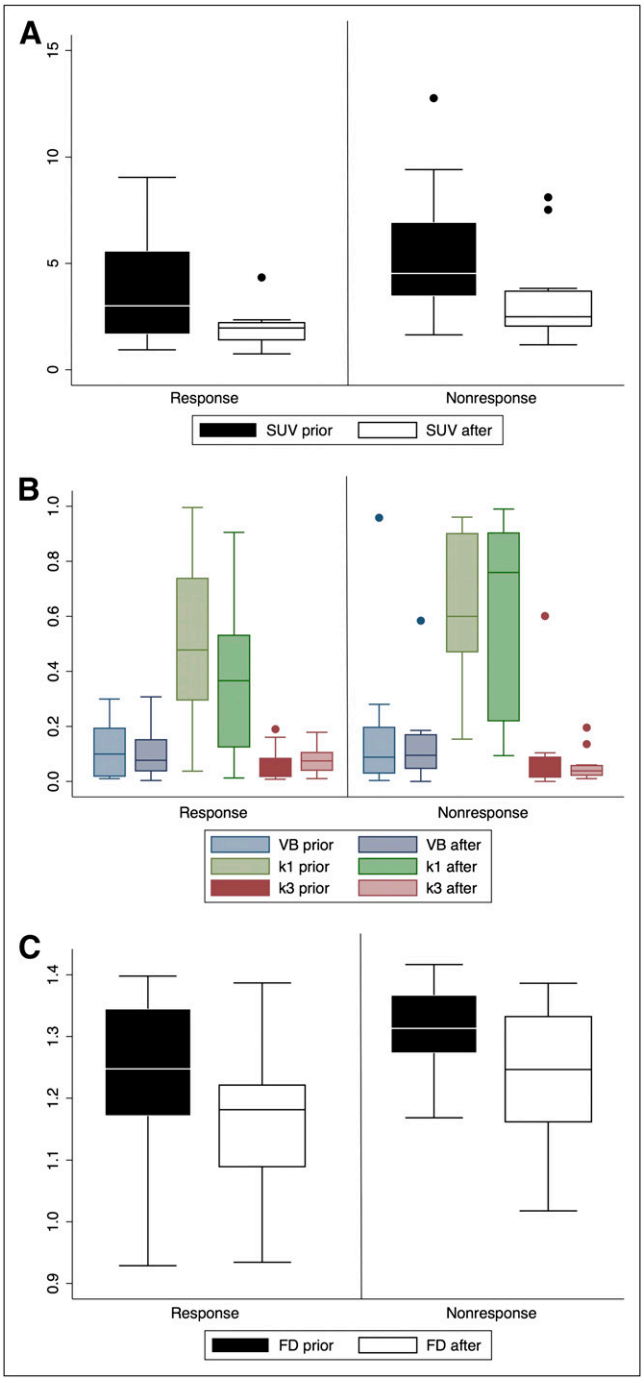

FIGURE 3. (A) Box-and-whisker plots of median tumor mean SUV 55–60 min after injection before and after 2 cycles of NAC in responders and nonresponders. (B) Box-and-whisker plots of median tumor values for VB, K_1, and k_3 before and after 2 cycles of NAC in responders and nonresponders. VB does not have units; K_1 and k_3 values are expressed in 1/min. (C) Box-and-whisker plots of median tumor FD before and after 2 cycles of NAC in responders and nonresponders.

Group-Based Classification According to Histopathologic Data by Use of Discriminant Analysis

The histopathologic response was classified as less than 10% viable tumor tissue. We categorized the patients (n = 25) according to this criterion and defined 2 response groups. Table 2 presents the results of the linear discriminant analysis with equal prior probabilities for each study and their combinations. The data demonstrate that the classification was generally higher (positive predictive value [PPV] > 67%) for the responders than for the nonresponders. The use of mean SUV and influx value was, in particular, high for the group of responders (PPV, 92%). Overall, the nonresponders could be best classified using the mean SUV and influx or the FD and k_4 of the follow-up study (negative predictive value, 83%). Finally, the combined use of the 2 predictor variables, namely mean SUV and influx, of each study led to the highest accuracy, 83%, for both groups. This combination was particularly useful for the prediction of responders (PPV, 92%). The use of the percentage change in maximum SUV (SUVmax) led to a sensitivity of 57%, a specificity of 60%, and an accuracy of 58%.

DISCUSSION

^{18}F-FDG imaging greatly affects the diagnostics and management of oncologic patients, in particular those who have a solid tumor. The impact of the predictive value of ^{18}F-FDG PET early in the course of chemotherapy is still open and under evaluation. Only a few reports exist on therapy monitoring of NAC in sarcomas using ^{18}F-FDG PET. The main difference between these studies and ours is the early time chosen for the follow-up in our design, consistent scheme for NAC, and data evaluation. The primary clinical demand is to assess the cytostatic effect early in the course of NAC to exclude nonresponders or modify the therapeutic protocol accordingly. Benz et al. reported on a study with 20 patients with locally advanced high-grade STSs who had been studied with ^{18}F-FDG PET/CT before and after the completion of the preoperative therapy, which included different chemotherapeutic protocols; 70% of the patients underwent additional external-beam radiation (*12*). The authors reported significant differences in SUV changes (mean and maximum) in histopathologic responders (70%−78%), as compared with the nonresponders (27%−40%). Histopathologic response was defined as less than 5% viable tumor tissue. In contrast, the changes in tumor volume as measured by CT did not allow the prediction of response. One limitation of this study is that only 6 of 20 patients were responders, which may raise statistical problems regarding the accuracy. Evilevitch et al. reported on a similar study including 42 patients with resectable high-grade sarcomas who received combined NAC and underwent ^{18}F-FDG PET/CT before and after the completion of NAC (*13*). Also in this study, NAC was not consistent, and 57% of the patients received additional external-beam radiation. The authors reported on a greater

TABLE 2. Results of Linear Discriminant Analysis with Equal Prior Probabilities Based on ^{18}F-FDG Parameters of First PET Study (1) or Second PET Study (2) or Combination of Both Studies

Parameter	Sensitivity	Specificity	PPV	NPV	Accuracy
1: SUV	9/15 (60.00%)	7/10 (70.00%)	9/12 (75.00%)	7/13 (54.00%)	16/25 (64.00%)
1: SUV, VB, k1, k3, FD	9/11 (81.81%)	3/14 (21.43%)	9/12 (75.00%)	10/13 (77.00%)	19/25 (76.00%)
2: SUV	10/16 (62.5%)	6/8 (75.00%)	10/12 (83.33%)	6/12 (50.00%)	16/24 (66.70%)
2: SUV, influx	8/9 (88.90%)	6/10 (60.00%)	8/12 (67.00%)	10/12 (83.30%)	18/24 (75.00%)
2: FD, k4	9/11 (81.81%)	3/13 (23.00%)	9/12 (75.00%)	10/12 (83.30%)	19/24 (79.20%)
1 + 2: SUV	9/14 (64.30%)	7/10 (70.00%)	9/12 (75.00%)	7/12 (58.33%)	16/24 (66.70%)
1 + 2: SUV, influx	11/14 (78.60%)	9/10 (90.00%)	11/12 (91.67%)	9/12 (75.00%)	20/24 (83.33%)
% change SUVmax	8/14 (57.14%)	6/10 (60.00%)	8/12 (66.67%)	6/12 (50.00%)	14/24 (58.33%)

Groups were defined according to histologic classification of 10% variable tumor tissue.
PPV = positive predictive value; NPV = negative predictive value.

reduction in ^{18}F-FDG uptake in histopathologic responders, whereas no significant changes were found for the tumor size. The best cutoff level for the assessment of histopathologic response was 60% decrease in tumor ^{18}F-FDG uptake, which led to a sensitivity of 100% and a specificity of 71%. The results demonstrate that a simple cutoff level for the change in SUV is related to low specificity. In contrast, Response Evaluation Criteria in Solid Tumors provided a sensitivity of 25% and a specificity of 100%. In our study, sensitivity was 78.6% and specificity 90% when using the absolute values of mean SUV and influx of both studies, compared with 64% and 70% when using only the mean SUVs of both studies. In particular, PPV (92%) and accuracy (83%) were highest when using the combination of mean SUV and influx of both studies. The data support the use of dPET, which is a prerequisite for the calculation of kinetic data for the prediction of therapy outcome. Because early measurements within NAC in sarcoma patients—as compared with measurements within a longer time interval and after several chemotherapeutic cycles in sarcoma patients—deal with smaller changes in the ^{18}F-FDG metabolism, the use of dPET and calculation of kinetic data seem to be helpful.

Some authors reported good results in other tumor types by performing a baseline and 1 follow-up study early in the course of NAC, within the first cycle. A reduction in ^{18}F-FDG uptake early in the course of NAC (14 d after onset) was a good prognostic criterion for the histopathologic response classification of tumors in the esophagogastric junction and was characterized by significantly longer time to progression and longer overall survival (*14*). The reported sensitivity was 89% and specificity was 75% with respect to the histopathologic response using a cutoff value of 35% reduction in ^{18}F-FDG metabolism, as compared with 57% sensitivity and 60% specificity for the percentage change in SUVmax, in our study. This may be related to the different histology and chemotherapeutic protocol used. The literature data concerning the change in ^{18}F-FDG uptake after chemotherapy and long-term therapy outcome are divergent. Schuetze et al. demonstrated in patients with localized extremity STSs treated with NAC that less than 40% decrease in SUVmax was a bad prognostic criterion, because these patients were at high risk of systemic disease recurrence estimated to be 90% at 4 y from the initial diagnosis (*15*). The main problem of the use of percentage change of ^{18}F-FDG metabolism is that sensitivity and specificity depend on the cutoff level used for discrimination, and dependence on cutoff level is furthermore dependent on the tumor histology and therapy used. The greater the percentage of ^{18}F-FDG reduction, the better the therapeutic result, as shown in different studies (*16,17*). Cerfolio et al. recommended the use of a decrease of more than 80% in SUVmax for the prediction of complete pathologic response, with a sensitivity of 90%, specificity of 100%, and accuracy of 96% in patients with non–small cell lung tumors who received NAC (*18*). In our study, the change in SUVmax led to a sensitivity of 57% and a specificity of 60% and was worse than the combination of the absolute mean SUV and influx values of both studies.

Most of the studies about monitoring the chemotherapeutic effect using PET in oncologic patients are based on simple quantification methods for data analysis. Most authors used only a visual or a semiquantitative method, for example, SUV or tumor–to–normal-tissue ratio. The use of SUV for the quantification of ^{18}F-FDG studies is a robust parameter that reflects tumor viability and has a prognostic value. Nonresponders demonstrated higher mean SUVs in the baseline study (5.5 vs. 3.9) as shown in the present study (Supplemental Table 1a) and as reported in the literature (*8,12,15*). Therefore, baseline ^{18}F-FDG uptake may have a prognostic value. Schuetze et al. demonstrated in patients with localized extremity STSs treated with NAC that a pretreatment tumor SUVmax greater than 6 was a bad prognostic criterion because these patients were at high risk of systemic disease recurrence estimated to be 90% at 4 y from the initial diagnosis (*15*). We reported that higher baseline ^{18}F-FDG metabolism as expressed in mean SUV or k_3 or FD in patients with non–small cell lung cancer was related to a shorter progression-free survival after chemo-

therapy (*7*). In patients with colorectal liver metastases, baseline mean SUVs greater than 6 were associated with an overall survival of less than 200 d after cytostatic treatment (*19*). The question is, however, how reliable is baseline mean SUV or its change for a response classification? Larson et al. proposed the use of another semiquantitative index of total tumor glycolysis (TLG) for better describing response to treatment (*20*). TLG is calculated by multiplying the CT volume and the SUV. However, because of the relatively small changes of tumor volume related to the presence of necrosis, edema, or hemorrhage—in particular early after chemotherapy—the use of TLG for early monitoring is doubtful as demonstrated in the study of Benz et al. (*12*). The authors demonstrated that the use of TLG diminished the histopathologic response information. Therefore, the use of TLG cannot be recommended on the basis of the literature data available.

Full dynamic quantitative studies provide the possibility of extending quantification and getting data about the ^{18}F-FDG kinetics. The hypothesis is that different time–activity curves of ^{18}F-FDG can achieve the same SUV as measured by a single static measurement 55–60 min after injection. However, by applying compartmental and noncompartmental analysis to the dynamic data, the shape of the time–activity curve is characterized, and therefore additional valuable information concerning the distribution volume VB (which is related to perfusion), influx and efflux of the tracer, and phosphorylation and dephosphorylation rate can be obtained. According to the results of the present study, the influx data were helpful, particularly in combination with SUV for the correct response classification. The calculation of influx comprises K_1, k_2, and k_3, which are the major compartment parameters. One problem that should be discussed is whether the use of just 1 parameter of the ^{18}F-FDG kinetics, such as the transport rates, is enough for an accurate prediction of response. Although nonresponders demonstrated higher mean SUV, FD, VB, and K_1–k_3 values before therapy (Supplemental Table 1b), the difference was not statistically significant. In the follow-up study, we found significant differences at a level of P less than 0.1 for K_1, k_4, and FD. Nonresponders were related to higher influx values, lower phosphorylation rates, and higher FD values after NAC. However, the presented data demonstrate that the best results for a group-based analysis, into responders and nonresponders, were obtained on the basis of a multiparameter analysis including the absolute values of mean SUV and influx of the baseline study and the follow-up study. The data demonstrate that EIA therapy may have a combined effect on both the angiogenesis and the proliferation because of the more pronounced effect on SUV and influx, which is a parameter that takes into account K_1, k_2, and k_3. In particular, the prediction of response was better (92%) based on the combination of the kinetic data, in comparison to the use of mean SUV alone (75%). The use of the percentage change of SUVmax cannot be recommended on the basis of the results of this study. Another major limitation of the use of SUVmax is that it is highly dependent on the statistical quality of the images and the size of the maximal pixel and is, therefore, less robust than the use of the average SUV within a VOI (*21*). The data give evidence for an assessment of the inhibitory effects of this type of chemotherapy using full kinetic analysis of the ^{18}F-FDG data of the baseline study and the study after the completion of 2 cycles of NAC.

CONCLUSION

Prediction of preoperative response is a topic that raises several questions concerning the handling of the data. The data of this study demonstrate that only a multiparameter analysis including the combination of the mean absolute values of mean SUV and influx of a baseline study and a follow-up study after completion of 2 cycles of NAC is a robust combination for a group-based analysis (of categorizing patients into response or nonresponse). The quantitative assessment of the ^{18}F-FDG kinetics in tumors should be used to measure the inhibitory effect of the chemotherapy on the tumor growth. In particular, the presented methodology may be used in patients with high-risk STSs, because proper selection of those patients who may benefit from a neoadjuvant chemotherapeutic treatment early in the course of treatment is necessary.

REFERENCES

1. National Cancer Institute. Soft Tissue Sarcomas: Questions and Answers. Available at: http://www.cancer.gov/cancertopics/factsheet/sites-types/soft-tissue-sarcoma. Accessed January 25, 2010.
2. Grobmyer SR, Maki RG, Demetri GD, et al. Neo-adjuvant chemotherapy for primary high-grade extremity soft tissue sarcoma. *Ann Oncol.* 2004;15:1667–1672.
3. Salzer-Kuntschik M, Brand G, Delling G. Determination of the degree of morphological regression following chemotherapy in malignant bone tumors. *Pathologe.* 1983;4:135–141.
4. Strauss LG, Conti PS. The applications of PET in clinical oncology. *J Nucl Med.* 1991;32:623–648.
5. Burger C, Buck A. Requirements and implementations of a flexible kinetic modeling tool. *J Nucl Med.* 1997;38:1818–1823.
6. Mikolajczyk K, Szabatin M, Rudnicki P, Grodzki M, Burger C. A Java environment for medical image data analysis: initial application for brain PET quantitation. *Med Inform (Lond).* 1998;23:207–214.
7. Dimitrakopoulou-Strauss A, Hoffmann M, Bergner R, et al. Prediction of short-term survival in patients with advanced nonsmall cell lung cancer following chemotherapy based on 2-deoxy-2-(F-18)-fluoro-D-glucose positron emission tomography: a feasibility study. *Mol Imaging Biol.* 2007;9:308–317.
8. Miyazawa H, Osmont A, Petit-Taboue MC, et al. Determination of ^{18}F-fluoro-2-deoxy-D-glucose rate constants in the anesthetized baboon brain with dynamic positron tomography. *J Neurosci Methods.* 1993;50:263–272.
9. Sokoloff L, Smith CB. Basic principles underlying radioisotopic methods for assay of biochemical processes in vivo. In: Greitz T, Ingvar DH, Widén L, eds. *The Metabolism of the Human Brain Studied with Positron Emission Tomography.* New York, NY: Raven Press; 1983:123–148.
10. Ohtake T, Kosaka N, Watanabe T, et al. Noninvasive method to obtain input function for measuring glucose utilization of thoracic and abdominal organs. *J Nucl Med.* 1991;32:1432–1438.
11. Dimitrakopoulou-Strauss A, Strauss LG, Mikolajczyk K, et al. On the fractal nature of positron emission tomography (PET) studies. *World J Nucl Med.* 2003;2:306–313.
12. Benz MR, Allen-Auerbach MS, Eilber FC, et al. Combined assessment of metabolic and volumetric changes for assessment of tumor response in patients with soft-tissue sarcomas. *J Nucl Med.* 2008;49:1579–1584.

13. Evilevitch V, Weber WA, Tap WD, et al. Reduction of glucose metabolic activity is more accurate than changes in size at predicting histopathologic response to neoadjuvant therapy in high-grade soft-tissue sarcomas. *Clin Cancer Res.* 2008; 14:715–720.
14. Weber WA, Ott K, Becker K, et al. Prediction of response to preoperative chemotherapy in adenocarcinomas of the esophagogastric junction by metabolic imaging. *J Clin Oncol.* 2001;19:3058–3065.
15. Schuetze SM, Rubin BP, Vernon C, et al. Use of positron emission tomography in localized extremity soft tissue sarcoma treated with neoadjuvant chemotherapy. *Cancer.* 2005;103:339–348.
16. Tseng J, Dunnwald LK, Schubert EK, et al. ^{18}F-FDG kinetics in locally advanced breast cancer: correlation with tumor blood flow and changes in response to neoadjuvant chemotherapy. *J Nucl Med.* 2004;45:1829–1837.
17. Hellwig D, Graeter TP, Ukena D, Georg T, Kirsch CM, Schäfers HJ. Value of F-18-fluorodeoxyglucose positron emission tomography after induction therapy of locally advanced bronchogenic carcinoma. *J Thorac Cardiovasc Surg.* 2004; 128:892–899.
18. Cerfolio RJ, Bryant AS, Winokur TS, Ohja B, Bartolucci AA. Repeat FDG-PET after neoadjuvant therapy is a predictor of pathologic response in patients with non-small cell lung cancer. *Ann Thorac Surg.* 2004;78:1903–1909.
19. Dimitrakopoulou-Strauss A, Strauss LG, Burger C, et al. Prognostic aspects of ^{18}F-FDG PET kinetics in patients with metastatic colorectal carcinoma receiving FOLFOX chemotherapy. *J Nucl Med.* 2004;45:1480–1487.
20. Larson SM, Erdi Y, Akhurst T, et al. Tumor treatment response based on visual and quantitative changes in global tumor glycolysis using PET-FDG imaging: the visual response score and the change in total lesion glycolysis. *Clin Positron Imaging.* 1999;2:159–161.
21. Boellaard R, Krak NC, Hoekstra OS, Lammertsma AA. Effects of noise, image resolution, and ROI definition on the accuracy of standard uptake values: a simulation study. *J Nucl Med.* 2004;45:1519–1527.

JNM The Journal of NUCLEAR MEDICINE

Impact of Dynamic ^{18}F-FDG PET on the Early Prediction of Therapy Outcome in Patients with High-Risk Soft-Tissue Sarcomas After Neoadjuvant Chemotherapy: A Feasibility Study

Antonia Dimitrakopoulou-Strauss, Ludwig G. Strauss, Gerlinde Egerer, Julie Vasamiliette, Gunhild Mechtersheimer, Thomas Schmitt, Burkhard Lehner, Uwe Haberkorn, Philipp Stroebel and Bernd Kasper

J Nucl Med. 2010;51:551-558.
Doi: 10.2967/jnumed.109.070862

The Journal of Nuclear Medicine is published monthly.
SNMMI | Society of Nuclear Medicine and Molecular Imaging
1850 Samuel Morse Drive, Reston, VA 20190.
(Print ISSN: 0161-5505, Online ISSN: 2159-662X)

SNMMI SOCIETY OF NUCLEAR MEDICINE AND MOLECULAR IMAGING